

Short Report

Fountain of youth for squamous cell carcinomas? On the epigenetic age of non-small cell lung cancer and corresponding tumor-free lung tissues

Sebastian Marwitz^{1,7}, Lena Heinbockel^{1,7}, Swetlana Scheufele^{2,7}, Christian Kugler³, Martin Reck^{4,7}, Klaus F. Rabe^{5,7}, Sven Perner¹, Torsten Goldmann^{1,7} and Ole Ammerpohl^{6,7}

¹Pathology of the University Medical Center Schleswig-Holstein (UKSH), Campus Luebeck and the Research Center Borstel, site Borstel, Germany

²Institute of Human Genetics, University Medical Center Schleswig-Holstein (UKSH), Campus Kiel, Germany

³Surgery, LungenClinic Grosshansdorf, Grosshansdorf, Germany

⁴Oncology, LungenClinic Grosshansdorf, Grosshansdorf, Germany

⁵Pneumology, LungenClinic Grosshansdorf, Grosshansdorf, Germany

⁶Institute of Human Genetics, University Medical Center Ulm, Ulm, Germany

⁷Airway Research Center North, Member of the German Center for Lung Research (DZL), Großhansdorf, Germany

Aging affects the core processes of almost every organism, and the functional decline at the cellular and tissue levels influences disease development. Recently, it was shown that the methylation of certain CpG dinucleotides correlates with chronological age and that this epigenetic clock can be applied to study aging-related effects. We investigated these molecular age loci in non-small cell lung cancer (NSCLC) tissues from patients with adenocarcinomas (AC) and squamous cell carcinomas (SQC) as well as in matched tumor-free lung tissue. In both NSCLC subtypes, the calculated epigenetic age did not correlate with the chronological age. In particular, SQC exhibited rejuvenation compared to the corresponding normal lung tissue as well as with the chronological age of the donor. Moreover, the younger epigenetic pattern was associated with a trend toward stem cell-like gene expression patterns. These findings show deep phenotypic differences between the tumor entities AC and SQC, which might be useful for novel therapeutic and diagnostic approaches.

Introduction

Life is limited by the progressive functional decline of the organism at multiple levels that is known as aging and that is, for most organisms, inevitable, and irreversible,^{1,2} with a few exceptions where negligible senescence can occur.³

Humans develop a plethora of age-related pathologies that lead to diseases such as atherosclerosis, osteoporosis, pulmonary insufficiency, and cancer.¹ Changes during the process of aging are not only limited to cellular functions, morphological changes or impaired organelles but also extend to the

Key words: non-small cell lung cancer, aging, epigenetic clock, stem cells, methylome, transcriptome

Abbreviations used: NSCLC: Non-small cell lung cancer; AC: adenocarcinoma; SQC: squamous cell carcinoma; DNAm age: epigenetic age; CSCs: cancer stem cells; iPSCs: induced-pluripotent stem cells

SM and LH share first authorship.

TG and OA share senior authorship.

Grant sponsor: Bundesministerium für Bildung und Forschung; **Grant numbers:** 01EY1103DZL; 82DZL001A5; **Grant sponsor:** Deutsche Forschungsgemeinschaft; **Grant numbers:** DR797/3-1; **Grant sponsor:** German Center for Lung Research; **Grant numbers:** 82DZL001A5; **Grant sponsor:** BioMaterialBank North; **Grant sponsor:** Airway Research Center North, German Center for Lung Research; **Grant sponsor:** German Ministry for Education and Research; **Grant numbers:** 01EY1103

This is an open access article under the terms of the Creative Commons Attribution-NonCommercial-NoDerivs License, which permits use and distribution in any medium, provided the original work is properly cited, the use is non-commercial and no modifications or adaptations are made.

DOI: 10.1002/ijc.31641

History: Received 26 Jan 2018; Accepted 25 May 2018; Online 4 Jul 2018

Correspondence to: Torsten Goldmann, Pathology Department of the University Medical Center Schleswig-Holstein (UKSH), Luebeck Campus and the Borstel Research Center, Lübeck, Germany, Parkallee 3a, 23845 Borstel, Germany, E-mail: tgoldmann@fz-borstel.de;

Fax: +49-4537-1882290

What's new?

Chronological age is correlated with the methylation status of CpG sites in the genome, enabling the study of aging-related phenomena. Here, investigation of molecular age loci in cells from patients with non-small cell lung cancer (NSCLC) reveals remarkable differences in NSCLC cell epigenetic age compared to the host's chronological age. Adenocarcinomas showed a higher epigenetic age than squamous cell carcinomas (SQC). Reduced SQC epigenetic age was accompanied by increased expression of stem cell gene signatures, suggesting an increased abundance of stem cells in SQC. Elevated stem cell levels could have clinical implications, as stem cells often show therapeutic resistance.

epigenome level and are likely influenced by epigenetic changes.²

The cytosine-5 methylation status of CpG sites can be used to estimate the epigenetic age (DNAm age) and to define an epigenetic clock, referred to as Horvath's clock, which correlates with the chronological age of the organism in multiple tissues. Interestingly, the calculated DNAm age is reduced in embryonic and induced-pluripotent stem cells and correlates well with the cell passage number.⁴ Moreover, different tumor types display DNAm age alterations and differ considerably from the chronological age of the host.^{4,5} Additionally, other CpG loci have been identified by correlation analyses to show age-dependent DNA methylation patterns.⁶

Here, we analyzed the DNAm age in a cohort of non-small cell lung cancer (NSCLC) samples and the corresponding tumor-free tissues to obtain insight into possible DNAm age changes and the underlying transcriptional processes.

Material and Methods**Sample origin**

Tissues from 33 patients who underwent surgery with curative intent due to lung cancer, composed of 15 adenocarcinomas (AC) and 18 squamous cell carcinomas, (SQC) were analyzed together with their matched tumor-free control tissues. Ethical permission was obtained from the University of Lübeck through BioMaterialBank North (Ref. 12–220). Tumor specimens were micro-dissected to enrich the tumor content for the methylome analysis⁷ and transcriptome analysis.⁸ For this, non-tumor content was scratched off the tissue sections under a microscope to deplete non-tumor cells and enrich NSCLC cells prior to the extraction of the nucleic acids.

Methylome analysis

After extraction of the DNA, methylome data was generated as previously reported using the HumanMethylation450K BeadChip (Illumina, Inc., San Diego, CA).⁷ Data were stored in the gene expression omnibus (GEO) (accession number GSE75008). CpG loci located on gonosomes as well as CpG loci with detection *P*-values > 0.01 in at least one sample were excluded from further analyses. Omics Explorer 3.2 (Qlucore, Lund, Sweden) was used for cluster analyses, principal component analysis (PCA) and data presentation.

To validate the results obtained from our cohort, DNA methylation data on lung adenocarcinoma (LUAD) and

squamous cell carcinoma (LUSC) made publicly available by The Cancer Genome Atlas (TCGA) project was included. The data was accessed from http://gdac.broadinstitute.org/runs/stddata__2014_09_02/data/ on December 1, 2017.

Calculation of DNA methylation age

Horvath's epigenetic clock is a method of predicting a specimen's age based on the DNA methylation values of the 353 CpG loci present on the HumanMethylation450K Bead-Chip. The epigenetic age (DNAm age) was calculated as described before⁴ using the DNAm age Calculator (accessible at <https://dnamage.genetics.ucla.edu/>).

Detection of aging-associated methylation regions

The DNA methylation profiles of 40 control lung specimens (chronological age 41–82 years; mean: 66 years, median: 66 years) were determined as described above. Using the R software package (version 3.4.1; www.r-project.org), Pearson's correlation coefficients of the donors' chronological ages and DNA methylation values (average beta values) were calculated for every CpG locus. CpG loci with absolute Pearson's correlation coefficients >0.6 were included in further analyses.

Transcriptome analysis

Gene expression data for 18 NSCLC tumors and matched tumor-free lungs from the GEO dataset GSE74706, for which methylome data (GSE75008) was also available, were selected for the transcriptome analysis and annotated with the difference in DNAm ages between the sample and the matched tumor-free lung (DNAm age [lung]—DNAm age [tumor]): 9495–10 (DNAm age diff: –37.6), 12097–07 (DNAm age diff: –25.5), 13230–12 (DNAm age diff: –23.9), 12928–12 (DNAm age diff: –23.7), 12799–12 (DNAm age diff: –10.8), 1888–12 (DNAm age diff: –9.3), 2508–11 (DNAm age diff: –5.3), 6495–08 (DNAm age diff: –1.1), 15982–07 (DNAm age diff: 15.5), 17962–08 (DNAm age diff: 27.6), 1799–12 (DNAm age diff: 31), 22024–11 (DNAm age diff: 34.2), 12893–12 (DNAm age diff: 37.4), 21918–11 (DNAm age diff: 38.3), 21577–08 (DNAm age diff: 44.3), 11560–12 (DNAm age diff: 51.5), 3302–12 (DNAm age diff: 62.1), and 5622–12 (DNAm age diff: 79.5). Samples were analyzed using GeneSpring software version 13.0 (Agilent Technologies, Böblingen, Germany) as described elsewhere.⁸ One-way ANOVA (1 W-ANOVA) was

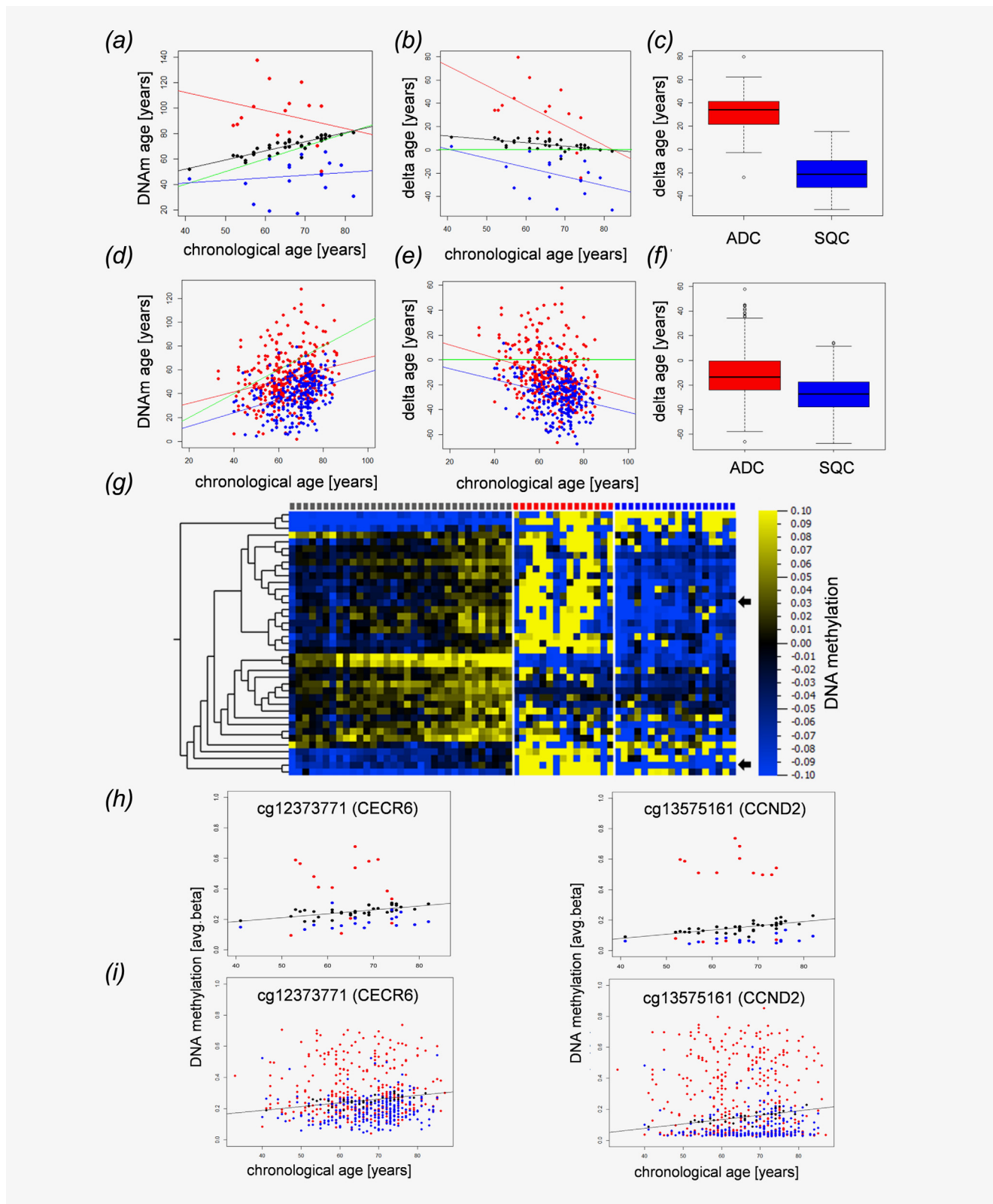


Figure 1. NSCLC tissues display epigenetic age distortions. Dot plot (a) and Bland–Altman-Plot (b) showing correlations between the chronological age of the host and the epigenetic DNAm age of matched tumor tissues from normal control specimens (black dots), adenocarcinomas (red) and squamous cell carcinomas (blue). (c) Boxplot of the deviations of DNAm age from the chronological age in adenocarcinomas (ADC, red) and squamous cell carcinomas (SQC, blue). The delta age of cancer entities differs significantly

(p -value $<1.32 \times 10^{-5}$, Wilcoxon rank sum test). Validation cohort (public available TCGA data set): Dot plot (*d*) and Bland–Altman-Plot (*e*) showing correlations between the chronological age and the epigenetic DNAm age of adenocarcinomas (red) and squamous cell carcinomas (blue) in an independent validation cohort. (*f*) The delta age of adenocarcinomas (ADC, red) and squamous cell carcinomas (SQC, blue) differs significantly (P -value $<2.2 \times 10^{-16}$, Wilcoxon rank sum test). The delta age is calculated as DNAm age (years)—chronological age (years). (*a, b, c, d*) Black, red and blue lines represent the regression lines for control samples, adenocarcinomas, and squamous cell carcinomas, respectively. The green line indicates a perfect match of chronological age and DNAm age (chronological age = DNAm age). DNA methylation changes of distinct CpG loci associated with aging and alterations of these patterns in lung cancer (*g–i*). Heatmap (*g*) of CpG loci with changing DNA methylation during aging. Pearson correlation analysis of avg. beta values of all CpG loci included in our study in normal lung tissue (controls) with the chronological age of the sample donors identified 39 loci with $|\text{Pearson correlation coefficients}| > 0.6$ (Table 1). The DNA methylation values of these loci are presented separately for controls (gray squares, top lane), adenocarcinoma (red squares) and squamous cell carcinoma (blue squares). Samples are ordered according to donors' chronological ages. Heatmap: blue, low DNA methylation values; yellow, high DNA methylation values, for visualization purposes, the DNA methylation values were normalized to zero for each locus, and the bar below the heatmap indicates the range and color code. Arrows indicate randomly selected loci detailed in H and I. (*h*) Detailed presentation of data from two randomly selected loci. DNA methylation of cg12373771 (CECR6) and cg13575161 (CCND2) increases during aging in control samples (black spheres). Compared to the controls, squamous cell carcinoma (blue spheres) are characterized by lower DNA methylation values, while DNA methylation is increased in adenocarcinoma (red spheres), putatively reflecting decelerated and accelerated aging, respectively. (*i*) A similar pattern is seen also in an independent dataset.

used for the analysis of >2 classes with a Benjamini-Hochberg multiple testing correction cut-off of $P \leq 0.05$ considered significant. Tukey post hoc testing was used for the selection of genes specific for each experimental condition. For unsupervised hierarchical clustering of normalized intensity values on genes and samples, the Pearson centered similarity measure was used together with Ward's linkage rule. Clusters were selected for further analysis by their distance metric, and gene symbols from each cluster were used to query the Molecular Signature Database (MSigDB) version 6 (<http://software.broadinstitute.org/gsea/msigdb>) for the enrichment of significant GO terms from biological processes, with an FDR q -value cut-off of $P \leq 0.05$ considered significant.

Gene set enrichment analysis (GSEA)

Gene set enrichment analysis (GSEA) software was downloaded from the BROAD Institute at <https://software.broadinstitute.org/gsea/index.jsp>. Next, 20 gene sets that contain stem cell gene expression signatures or genes that are upregulated in stem cells,⁹ regulate tumor stemness or are involved in embryonic stem cells were retrieved from the Molecular Signatures Database (MSigDB) and uploaded into the GSEA software. Normalized transcriptome data that contain the gene expression signatures of tumor samples with younger or older DNAm ages than the respective tumor-free lung samples were loaded into GSEA software, and the analysis was run with the default parameters. Normalized enrichment scores (NES) were used to retrieve genes with an enrichment of > 1 for detailed analysis and correlation with the DNAm age. Hierarchical clustering of selected genes from the GSEA was conducted using the Multi Experiment Viewer version 4 (<http://mev.tm4.org/>) with the Pearson centered algorithm. Selected genes and their normalized expression from the enrichment results were plotted against the DNAm age difference of each patient. A linear regression line was fitted, and the 95% confidence intervals were displayed. Pearson's correlation was conducted on plotted values using GraphPad Prism version 7.

Results and Discussion

Epigenetic analysis of NSCLC tissues revealed reduced DNAm age of SQC and accelerated DNAm age of AC

Given the accuracy of the Horvath clock's ability to reflect the host's age based on the methylation level, we investigated the DNAm age of NSCLC tissues and matched tumor-free lung tissues in comparison to their chronological ages. Overall, cancer tissues exhibited a different DNAm age than the tumor-free tissues. Furthermore, AC behaved differently than squamous cell carcinomas (SQC) (Fig. 1*a*) and seemed to have a higher DNAm age than the tumor-free lungs and an even more pronounced increased age compared to that of SQC. This was also true for the differences between the DNAm age of the tumors and the matched tumor-free tissues (Fig. 1*b*). Overall, SQC tissue exhibited a significantly decreased DNAm age compared to that of AC tissue (p -value $<1.32 \times 10^{-5}$, Fig. 1*c*) and their respective tumor-free tissues. Since the investigated dataset was comprised of a limited number of samples, we further investigated publicly available datasets from TCGA. In line with our data, SQC exhibited a significantly (P -value $<2.2 \times 10^{-16}$) lower delta age (DNAm age—chronological age) than that of AC specimens (Figs. 1*d–1f*). However, in contrast to our data set age acceleration in AC was detected only in some of the TCGA samples.

The DNAm age deviations from the chronological ages of the tumor-free lung tissues might be explained by the possible presence of COPD or smoking habits.¹⁰ Among these, patients showing an age acceleration of more than 8 years (7 cases) smoked 63.1 pack-years, while patients showing a deceleration of the DNAm age in the tumor-free lungs (3 cases) smoked 23.3 pack-years. There was no correlation between the pack-years, GOLD-grade, or emphysema and the DNAm age of the tumor-free lung tissues; however, it has been shown that DNAm age acceleration measured in the blood are predictive of various diseases including cancer.¹¹ The strongly decreased DNAm age of SQC (mean: 25.1 years) and the accelerated DNAm age of AC (mean + 25.9 years) raises questions about the underlying biological mechanisms.

Table 1. DNA methylation changes in distinct CpG loci associated with aging in normal lung tissue

TargetID	Chromosome	MAPINFO	UCSC refgene name	Pearson correlation coefficient
cg23040782	1	6762215	DNAJC11	0.6081
cg23813012	1	14026482	PRDM2	0.7119
cg08169949	1	28241532	RPA2	0.6041
cg12100751	1	109203672	C1orf59	0.6230
cg03105929	1	161591659		0.6254
cg02375320	2	38978881	SFRS7	0.6013
cg12206199	2	39187543	LOC375196	0.6168
cg23606718	2	131513927	FAM123C	0.6033
cg03545227	2	220173100	PTPRN	0.7443
cg07720856	2	232572668	PTMA	0.6784
cg12141030	3	44803447	KIAA1143	0.6760
cg07303143	3	44803452	KIAA1143	0.7257
cg10806820	3	48699090	CELSR3	0.6388
cg19614811	3	98250723	GPR15	0.6763
cg09401099	3	156534380		0.6094
cg05991454	4	147558435		0.6354
cg15936446	5	42952369		0.6168
cg04268670	5	76926341	OTP	0.6019
cg26921969	5	92948217		0.6318
cg03873281	5	131608955	PDLIM4	-0.6160
cg22736354	6	18122719	NHLRC1	0.6632
cg20899581	6	27841230	HIST1H4L	0.6873
cg20692569	7	72848481	FZD9	0.6563
cg21186299	7	100808810	VGF	0.6358
cg26830108	7	100813299		0.6216
cg05418199	8	6756832		0.6723
cg18245316	8	144962981		0.6002
cg14138050	9	14693504	ZDHHC21	0.6029
cg14506657	9	86755443		0.6481
cg08715791	11	66189297	NPAS4	0.6451
cg13575161	12	4381792	CCND2	0.7322
cg03036557	13	92050720	GPC5	0.6086
cg12678562	13	92050726	GPC5	0.6196
cg11082362	14	36003181	INSM2	0.6182
cg07850604	14	36003443	INSM2	0.6071
cg08151705	17	33775917	SLFN13	0.6324
cg04179438	17	75082479		-0.6289
cg07873590	19	17858298	FCHO1	0.6030
cg12373771	22	17601381	CECR6	0.6639

Age-related DNA methylation patterns are disturbed in lung carcinoma

In addition to Horvath's epigenetic clock, which relies on a comprehensive mathematical approach,⁴ additional age-related changes in the DNA methylation values of multiple genes have been described.⁶ Given the alterations in the Horvath loci, we wondered whether DNA methylation patterns directly relate to age, indicating aberrant epigenome aging in

NSCLC. Therefore, we determined the correlation coefficients between donors' chronological ages and the DNA methylation values for every CpG locus in 40 matched controls. In so doing, we identified 40 CpG loci with absolute Pearson's correlation coefficients > 0.6 (Fig. 1g). Of these, one locus (cg22901919; CLGN) was removed from further analysis due to insufficient data from the malignant specimens. The remaining 39 loci are allocated to 26 genes (Table 1). Many of these loci have been

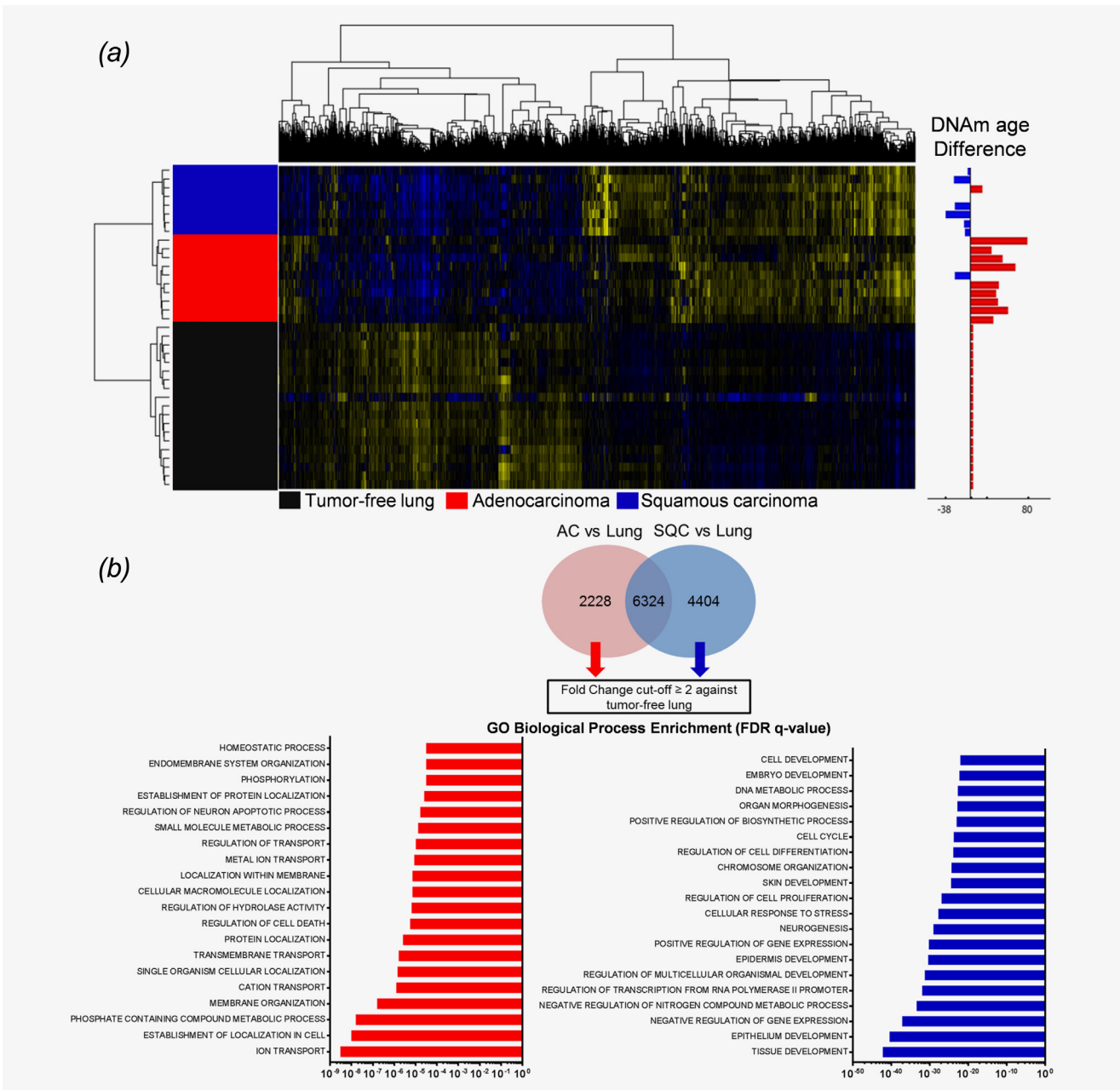


Figure 2. NSCLC tumors display a differential gene expression pattern associated with differentiation and developmental processes in SQC. (a) NSCLC tumors and matched tumor-free lungs were analyzed by 1 W-ANOVA for the significantly different expression of genes. The difference in DNAm age for each tumor compared to the chronological age of the host is displayed as an adjacent annotation track. Hierarchical clustering clearly separated all groups. (b) Specific gene expression signatures of AC and SQC tumors were derived from genes found to be significantly differentially expressed between adenocarcinomas and tumor-free lungs and between squamous cell carcinomas and tumor-free lungs, as indicated by the Tukey HSD post hoc test. From both gene lists, shared genes were excluded, and specific signatures were extracted. Only those genes with a fold-change of ≥ 2 compared to the tumor-free lung tissues were subjected to GO enrichment analysis. Gene Ontology analysis displays the top 20 most significantly enriched GO terms, as determined by the FDR q-values.

previously described as being either expressed or methylated in an age-related or disease-related manner in other tissues^{12,13} or as being affected in lung cancer.¹⁴ The 39 loci were significantly enriched for DNase I hypersensitive sites (DHS, OR = 5.541, RR = 5.540, $p < 0.0001$; chi-square test) and known

differentially methylated regions (DMR, OR = 8.873, RR = 8.869, $P < 0.0001$) according to array annotation, suggesting a possible role in gene regulation. Twenty-four (61.5%) of these loci were differentially methylated between SQC and their corresponding controls and the DNA methylation of 10 loci (25.6%)

(a)

NAME	SIZE	ES	NES	NOM p-val	FDR	FWER
BENPORATH_ES_CORE_NINE	6	0.76	0.76	0.07	0.06	0.036
BENPORATH_PROLIFERATION	74	0.63	0.63	0.08	0.19	0.208
BENPORATH_ES_1	154	0.53	0.53	0.01	0.21	0.396
BENPORATH_ES_2	8	0.56	0.56	0.24	0.21	0.339
CONRAD_STEM_CELL	16	0.57	0.57	0.02	0.26	0.326
WONG_EMBRYONIC_STEM_CELL_CORE	161	0.47	0.47	0.23	0.27	0.497
BHATTACHARYA_EMBRYONIC_STEM_CELL	44	0.43	0.43	0.31	0.34	0.6
BENPORATH_CYCLING_GENES	262	0.41	0.41	0.17	0.35	0.639
BENPORATH_NOS_TARGETS	73	0.36	0.36	0.05	0.38	0.726
BOQUEST_STEM_CELL_UP	129	0.37	0.37	0.39	0.39	0.704
BENPORATH_OCT4_TARGETS	118	0.32	0.32	0.09	0.49	0.797
RAMALHO_STEMNESS_UP	96	0.26	0.26	0.58	0.57	0.879
BENPORATH_EED_TARGETS	304	0.26	0.26	0.18	0.58	0.872
BENPORATH_NANOG_TARGETS	371	0.28	0.28	0.19	0.6	0.86
BENPORATH_SOX2_TARGETS	267	0.26	0.26	0.27	0.62	0.871
BENPORATH_PRC2_TARGETS	186	0.23	0.23	0.46	0.65	0.913
BENPORATH_ES_WITH_H3K27ME3	330	0.23	0.23	0.48	0.65	0.922
BENPORATH_SUZ12_TARGETS	309	0.19	0.19	0.77	0.83	0.967

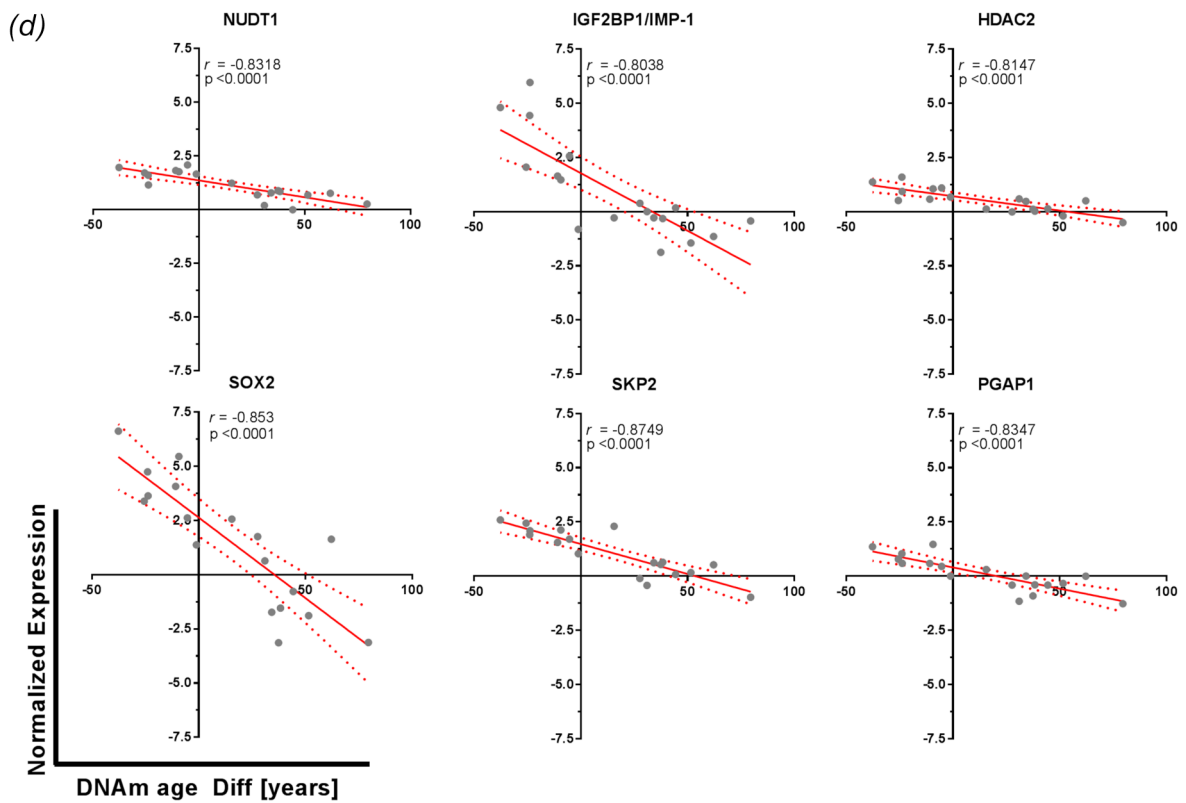
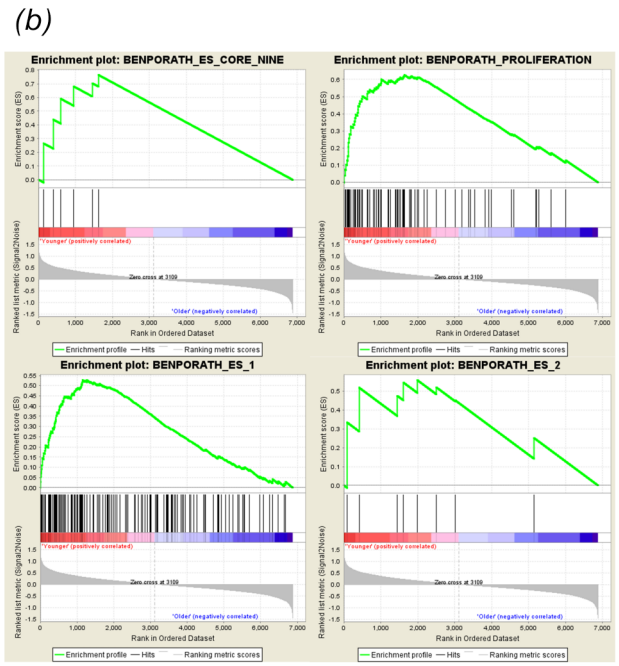
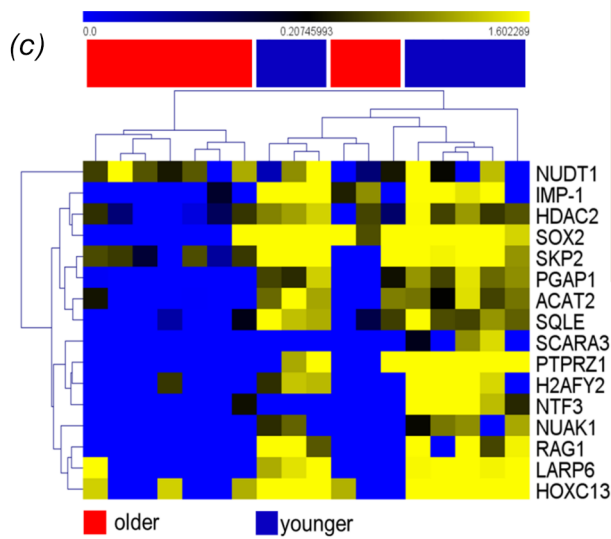


Figure 3. Epigenetically rejuvenated tumors display enriched stem cell gene signatures. (a) Transcriptome data of tumors with an accelerated or “older” and de-accelerated or “younger” DNAm ages compared to the chronological ages of the same patient’s tumor-free lung tissue were subjected to GSEA analysis. Twenty-one gene sets from the MSigDB that contained expression profiles of stem cells, stemness-related gene pattern, or embryonic stem cells were analyzed for possible enrichment within the dataset; 1/21 gene sets were filtered out by the gene set size filter (min = 5, max = 500). Of the remaining 20 gene sets, 18 were found to be upregulated in epigenetically younger tumors, and two were upregulated in epigenetically older tumors. (a) Summary table of GSEA analysis. ES, enrichment score, NES, normalized enrichment score, NOM *P*-val, nominal *P*-value, FDR, FDR *q*-value, FWER, family-wise error rate. (b) Enrichment plots of gene sets showing a trend to be regulated in younger tumors with an FDR <25%. (c) Hierarchical clustering of genes from the GSEA with a normalized enrichment score > 1 and their normalized gene expression within younger and older samples. (d) The top six genes according to the NES with enrichment of their normalized expression were plotted against the DNAm age difference between the tumor and the tumor-free lung tissue. The solid red line shows the best fit, and the dotted red lines indicate the 95% confidence intervals. Pearson’s correlation coefficients are shown in each quadrant.

differentiated between AC tissues and their corresponding controls, while 9 loci (23.1%) were differentially methylated between AC and SQC of the lung (Student’s *t*-test, two-sided). Interestingly, 22 of the loci that were aberrantly methylated in SQC showed DNA hypomethylation compared to the controls. Only two loci showed hypermethylation (cg12206199, cg15936446). In contrast, 6/10 aberrantly methylated loci in adenocarcinoma showed DNA hypermethylation compared to the corresponding controls. All loci differentially methylated between AC and SQC had lower methylation levels in SQC. As low DNA methylation at these loci is indicative of lower age (Figs 1g–1i), these findings support our conclusion that AC are “epigenetically older” than squamous cell carcinomas.

RNA expression levels of SQC/younger DNAm age patients and AC/older DNAm age patients reveal the underlying biological processes

To further decipher the processes that differentiate tumors with an accelerated DNAm age from tumors with a lower DNAm age, we investigated the transcriptome data of those samples for which DNAm age and gene expression data were available. Microarray data were annotated for the calculated DNAm age difference of each patient, and significantly differentially expressed genes were identified, separating AC from SQC and tumor-free lungs (Fig. 2a). Specific gene signatures attributed to either AC or SQC were extracted from the 1 W-ANOVA results (Fig. 2b). To identify the possible underlying processes, GO analysis was conducted on twofold upregulated genes, resulting in strikingly different outcomes. SQC/younger DNAm age samples exhibited various enriched terms for developmental processes such as “tissue development”, “regulation of multicellular organismal development” or “embryo development” (Fig. 2b), suggesting cell fate regulating processes. In contrast, AC/older DNAm age samples displayed enriched terms for metabolic activity such as “ion transport” or “homeostatic process”.

Stem cell signatures show a trend towards enrichment in tumor tissues classified younger in DNAm age

We next hypothesized that this increased activity of cell fate decisions or differentiation processes might be caused by stem

cell activity. Therefore, gene sets describing embryonic-like stem cell genes⁹ and others were investigated for enrichment between younger and older DNAm age patients. Both groups exhibited an enrichment of gene sets, with 18/20 found to be upregulated in epigenetically younger tumors compared to 2/20 upregulated in epigenetically older tumors. However, only four gene sets from the epigenetically younger tumors passed the generic GSEA FDR cut-off (< 0.25). These sets indicated a trend towards enrichment of stem cell signatures. The results from the GSEA are shown in Figure 3, with Figure 3a summarizing the enrichment results in epigenetically younger tumors. The significantly enriched gene sets and their enrichment plots are shown in Figure 3b. Here, the gene set “Benporath_Es_Core_Nine” contains embryonic stem cell transcription regulators that are also overexpressed in high-grade, ER-negative breast cancers, while “Benporath_Proliferation” contains crucial genes for proliferation. The gene sets “Benporath_ES_1 and ES_2” are the results of meta-analysis of genes found to be overexpressed in human embryonic stem cells from 5 out of 20 profiling studies. The enrichment plots in all gene sets show a positive correlation of matched hits with the samples of a younger DNAm age, as the hits aggregate on the left side of each curve (Fig. 3b). Next, those genes that displayed an NES of > 1 were selected for more detailed analyses. Hierarchical clustering of the expression patterns of these genes among the investigated tumors revealed a clear pattern. The enriched genes from the stem cell gene sets were found to be overexpressed and clustered with tumors of a younger DNAm age (Fig. 3c). The top six genes from this list of enriched genes were used to plot the normalized gene expression against each patient’s DNAm age difference. Linear regression was computed to insert a best fit line, and the data were correlated. All six genes showed significant and strong negative correlations with the DNAm age differences (Fig. 3d). The higher the expression levels of these genes were, the lower the calculated DNAm age difference between the tumor and the tumor-free lung. One of the enriched genes from the gene sets with a strong negative correlation with DNAm age was SOX2. SOX2 is involved in the pluripotency of human embryonic stem cells^{15,16} and is indicative of squamous histology¹⁷ as well as being an antagonist of the tumor-suppressive Hippo pathways, leading to maintenance of cancer stem cells¹⁸ (CSCs). This

observation might reflect the nature of lung SQC, exhibiting an increased stem cell activity accompanied by decreased DNAm age, as possible CSC populations have been identified in NSCLC cell lines and tissues,¹⁹ with SQC exhibiting a higher fraction of stem cells leading to speculation about the respective cells of origin.²⁰ Furthermore, embryonic or induced-pluripotent stem cells (iPSCs) have DNAm ages close to zero,⁴ which is, at least in part, mirrored by the observed reduced DNAm age in SQC, thereby further strengthening the observation. Whether increased stem cell activity or the processes leading to reduced DNAm age are causative during carcinogenesis or vice versa constitutes a question that might lead to future therapies, as active interference with the epigenome has gained widespread attention.²¹ Even more, these data might be reflected in the clinic by observations of SQC patients who exhibit lower 1-year survival²² or overall survival²³ rates compared to those of AC patients. CSCs display increased chemotherapy resistance,²⁴ hence contributing to the reduced effectiveness of chemotherapy for SQC.

Determination of the DNAm age of AC and SQC using Horvath's DNA Methylation Age Calculator revealed a markedly younger DNAm age for SQC tissue compared to matched tumor-free lung tissue from the same patients. AC tissue seem to show an increased epigenetic age, pointing to the distinctively different biological processes taking place or even having already taken place in the course of carcinogenesis.

Second, we identified loci showing age-related changes in DNA methylation patterns and subsequently compared those DNA methylation patterns with methylation patterns obtained from corresponding cancer samples. The vast majority of these loci were aberrantly hypomethylated in SQC compared to the controls. Since DNA methylation of these loci increases with age, this suggests either decelerated aging or rejuvenation. Moreover, all the differentially methylated loci between AC and SQC showed higher levels of DNA methylation in AC, which points to accelerated aging in AC.

References

- Campisi J. Aging, cellular senescence, and cancer. *Annual review of physiology* 2013;75:685–705.
- Booth LN, Brunet A. The aging epigenome. *Mol Cell* 2016;62:728–44.
- Kogan V, Molodtsov I, Menshikov LI, et al. Stability analysis of a model gene network links aging, stress resistance, and negligible senescence. *Sci Rep* 2015;5:13589.
- Horvath S. DNA methylation age of human tissues and cell types. *Genome biology* 2013;14:R115.
- Lin Q, Wagner W. Epigenetic aging signatures are coherently modified in cancer. *PLoS Genet* 2015; 11:e1005334.
- Hannum G, Guinney J, Zhao L, et al. Genome-wide methylation profiles reveal quantitative views of human aging rates. *Mol Cell* 2013;49: 359–67.
- Marwitz S, Kolarova J, Reck M, et al. The tissue is the issue: improved methylome analysis from paraffin-embedded tissues by application of the HOPE technique. *Lab Invest* 2014;94:927–33.
- Marwitz S, Depner S, Dvornikov D, et al. Downregulation of the TGFbeta pseudoreceptor BAMBI in non-small cell lung cancer enhances TGFbeta Signaling and Invasion. *Cancer research* 2016;76:3785–801.
- Ben-Porath I, Thomson MW, Carey VJ, et al. An embryonic stem cell-like gene expression signature in poorly differentiated aggressive human tumors. *Nat Genet* 2008;40: 499–507.
- Gao X, Zhang Y, Breitling LP, et al. Relationship of tobacco smoking and smoking-related DNA methylation with epigenetic age acceleration. *Oncotarget* 2016;7:46878–89.
- Perna L, Zhang Y, Mons U, et al. Epigenetic age acceleration predicts cancer, cardiovascular, and all-cause mortality in a German case cohort. *Clin Epigenetics* 2016;8:64.
- Lim SL, Qu ZP, Kortschak RD, et al. HENMT1 and piRNA stability are required for adult male germ cell transposon repression and to define the spermatogenic program in the mouse. *PLoS Genet* 2015;11:e1005620.
- Bacos K, Gillberg L, Volkov P, et al. Blood-based biomarkers of age-associated epigenetic changes in human islets associate with insulin secretion and diabetes. *Nat Commun* 2016;7:11089.
- Yoon KA, Park S, Hwangbo B, et al. Genetic polymorphisms in the Rb-binding zinc finger gene RIZ and the risk of lung cancer. *Carcinogenesis* 2007;28:1971–7.
- Adachi K, Suemori H, Yasuda SY, et al. Role of SOX2 in maintaining pluripotency of human embryonic stem cells. *Genes Cells* 2010;15: 455–70.

Although accelerated DNAm age has been already described in various cancer samples^{4,5,11} and has been linked to lung cancer risk,²⁵ our study is the first to report striking differences in DNAm age compared with that of the matched internal control tissues and to attribute reduced DNAm age to increased stem cell gene activity in SQC.

Acknowledgments

The authors thank Lorena Valles, Jasmin Tiebach, Maria Lammers, and Kristin Wiczkowski for excellent technical assistance.

Competing interests

The authors declare that they have no competing interests.

Declarations

Ethics approval and consent to participate

The use of patient material was approved by the local ethics council at the University of Lübeck (AZ-12-220).

Funding

This work was funded by the German Center for Lung Research (DZL; 82DZL001A5) and the Deutsche Forschungsgemeinschaft (DR797/3–1). Patient tissues were provided by BioMaterialBank North, which is funded in part by the Airway Research Center North (ARCN, which is a member of the German Center for Lung Research, DZL) and is a member of the popgen 2.0 network (P2N), which is supported by a grant from the German Ministry for Education and Research (01EY1103).

Authors' contributions

SM and LH drafted the manuscript and created the figures. OA conceived of the study. OA and SS prepared and analyzed the methylome data. SM analyzed the transcriptome data. TG, CK, MR, KR and SP edited the manuscript. All authors read and approved the final manuscript.

16. Bass AJ, Watanabe H, Mermel CH, et al. SOX2 is an amplified lineage-survival oncogene in lung and esophageal squamous cell carcinomas. *Nat Genet* 2009;41:1238–42.
17. Wilbertz T, Wagner P, Petersen K, et al. SOX2 gene amplification and protein overexpression are associated with better outcome in squamous cell lung cancer. *Mod Pathol* 2011;24:944–53.
18. Basu-Roy U, Bayin NS, Rattanakorn K, et al. Sox2 antagonizes the Hippo pathway to maintain stemness in cancer cells. *Nat Commun* 2015;6:6411.
19. Leung EL, Fiscus RR, Tung JW, et al. Non-small cell lung cancer cells expressing CD44 are enriched for stem cell-like properties. *PloS one* 2010;5:e14062.
20. Giangreco A, Groot KR, Janes SM. Lung cancer and lung stem cells: strange bedfellows? *Am J Respir Crit Care Med* 2007;175:547–3.
21. Jones PA, Issa JP, Baylin S. Targeting the cancer epigenome for therapy. *Nat Rev Genet* 2016;17:630–41.
22. Cetin K, Ettinger DS, Hei YJ, et al. Survival by histologic subtype in stage IV nonsmall cell lung cancer based on data from the surveillance, epidemiology and end results program. *Clin Epidemiol* 2011;3:139–48.
23. Kogure Y, Ando M, Saka H, et al. Histology and smoking status predict survival of patients with advanced non-small-cell lung cancer. Results of West Japan oncology group (WJOG) study 3906L. *J Thorac Oncol* 2013;8:753–8.
24. Dean M, Fojo T, Bates S. Tumour stem cells and drug resistance. *Nat Rev Cancer* 2005;5:275–84.
25. Levine ME, Hosgood HD, Chen B, et al. DNA methylation age of blood predicts future onset of lung cancer in the women's health initiative. *Aging (Albany NY)* 2015;7:690–700.